Pharm Res (2014) 31:3335–3347
DOI 10.1007/s11095-014-1423-2

RESEARCH PAPER

Controlled Delivery of Fibroblast Growth Factor-9 from Biodegradable Poly(ester amide) Fibers for Building Functional Neovasculature

Somiraa S. Said • J. Geoffrey Pickering • Kibret Mequanint

Received: 5 March 2014 / Accepted: 12 May 2014 / Published online: 24 May 2014

ABSTRACT

Purpose For building functional vasculature, controlled delivery of fibroblast growth factor-9 (FGF9) from electrospun fibers is an appealing strategy to overcome challenges associated with its short half-life. FGF9 sustained delivery could potentially drive muscularization of angiogenic sprouts and help regenerate stable functional neovasculature in ischemic vascular disease patients.

Methods Electrospinning parameters of FGF9-loaded poly(ester amide) (PEA) fibers have been optimized, using blend and emulsion electrospinning techniques. *In vitro* PEA matrix degradation, biocompatibility, FGF9 release kinetics, and bioactivity of the released FGF9 were evaluated. qPCR was employed to evaluate platelet-derived growth factor receptor-β (PDGFRβ) gene expression in NIH-3T3 fibroblasts, 10T1/2 cells, and human coronary artery smooth muscle cells cultured on PEA fibers at different FGF9 concentrations.

Results Loaded PEA fibers exhibited controlled release of FGF9 over 28 days with limited burst effect while preserving FGF9 bioactivity. FGF9-loaded and unloaded electrospun fibers were found to support the proliferation of fibroblasts for five days even in serum-depleted conditions. Cells cultured on FGF9-supplemented PEA mats resulted in upregulation of PDGFRβ in concentration and cell type-dependent manner.

Conclusion This study supports the premise of controlled delivery of FGF9 from PEA electrospun fibers for potential therapeutic angiogenesis applications.

KEY WORDS Electrospinning · Fibroblast growth factor-9 · Poly(ester amide)s · Therapeutic angiogenesis

INTRODUCTION

Ischemic vascular diseases are characterized by inadequate delivery of blood and oxygen to tissues; coronary artery disease affects the heart, cerebrovascular disease affects the brain, and the peripheral arterial disease affects skeletal muscles and other internal organs (1). The principal pathological process causing ischemic diseases is atherosclerosis, which is a progressive inflammatory condition that usually affects large arteries, in which the accumulation of lipids, inflammatory cells, and fibrous material in the inner arterial wall results in the occlusion of these arteries (2). Many ischemic disease patients are ineligible for standard revascularization techniques due to poor overall health status or underlying comorbidities. Furthermore, a significant percentage of patients undergoing revascularization procedures do not meet the desired treatment outcome or experience restenosis, resulting in a poor prognosis and diminished quality of life, necessitating novel therapeutic alternatives for treatment of ischemic diseases (1).

Therapeutic angiogenesis, which includes the administration of growth factors for new and stable blood vessel formation, is an appealing approach to simulate angiogenesis in order to improve tissue perfusion and accelerate tissue regeneration in several pathological conditions such as ischemic heart disease, critical limb ischemia, diabetic ulcers, and delayed wound healing, leading to the functional recovery of ischemic tissues. However, the short half-life of exogenously delivered growth factors results in their rapid clearance from

S. S. Said
Biomedical Engineering Graduate Program
The University of Western Ontario, London, Ontario, Canada

J. G. Pickering
Department of Medicine (Cardiology), Department of Biochemistry, and Department of Medical Biophysics
The University of Western Ontario, London, Ontario, Canada

K. Mequanint (✉)
Department of Chemical and Biochemical Engineering and Biomedical Engineering Graduate Program, The University of Western Ontario, 1151 Richmond Street, London, Ontario N6A 5B9, Canada
e-mail: kmequani@uwo.ca

the application site following their delivery in a soluble form as an injection or infusion in the systemic circulation or tissue of interest (3). One approach to overcome such limitations is the controlled delivery of growth factors at the desired site from fibers using either blend, coaxial or emulsion electrospinning techniques (4–7). This can boost the stability of the growth factors and enable the sustained release of angiogenic factors in a biologically active form at the site of interest (8).

Fibroblast factor-9 (FGF9) or glial activating factor is one of the FGF superfamily and relatively little is known regarding its physiological function (9). It has higher specificity to fibroblast growth factor receptor–2/–3 isoforms (9–11), and was shown to demonstrate an elevated neointimal expression after arterial injury and contributes to smooth muscle cell proliferation (10). Recently, it has been reported that even though FGF9 did not itself stimulate angiogenesis, it was found to drive muscularization of angiogenic sprouts and that its delivery imparts stability, longevity, and the ability to regulate blood flow through vasoresponsiveness to newly formed microvessels (12). The FGF9-induced layering of neovessels was suggested to be mediated by sonic hedgehog-PDGFRβ-dependent signaling and it enhanced the ability of the neovasculature to receive flow and resist regression (12). FGF9 delivery by means of an osmotic pump to ischemic hind limbs promoted neovascular maturation and recovery of limb function (12). Therefore, FGF9 delivery may be required in order to drive the angiogenesis process towards completion since angiogenic growth factors by themselves cannot efficiently produce vasoreactive neovessels (13). Controlled-release biodegradable polymeric fibers can serve as a simple, low-cost and efficient alternative for implantable mini-infusion pumps for the delivery of FGF9, without the need of delivery system removal after consumption of the growth factor.

Poly(ester amide)s (PEAs), successfully synthesized in our laboratory, are protein-analog polymers that were found to have the potential to promote vascular tissue regeneration owing to their biomimetic properties and favorable degradation profiles (14), for which bioactive molecules can be incorporated, potentially sustaining their release, enhancing their efficacy, and accelerating favorable cell-material interactions. Degradation products of PEAs derived from naturally occurring α-amino acids are nontoxic and can be well metabolized by the body. Moreover, PEAs degradation is not accompanied by the release of acidic by-products, thus avoiding pH decrease in the vicinity of the scaffold, usually resulting in inflammatory responses (15). Nevertheless, surface eroding PEA scaffolds exhibit linear drug release kinetics (16), which provides better control of the drug release profile. Although electrospinning of a small number of PEAs have been reported (17–19), these PEA fibers were either prepared from low-molecular weight PEAs resulting in large diameter-fibers (from 0.64 to 3.5 μm) (17), or a polymer blend was required for electrospinning, where polycaprolactone was added to L-alanine-based PEA as a viscosity modifier to facilitate electrospinning (18). Moreover, *in vitro* degradation studies of other alanine-based PEA electrospun fibers showed that they were not practically degradable, where the weight loss was less than 6% after 305 days of incubation in phosphate buffered saline at 37°C (19).

In this study, amino acid-based biodegradable protein-analog electrospun PEA fibers have been fabricated for controlled delivery of growth factors intended for therapeutic angiogenesis applications. Our goal here is to prepare FGF9-loaded protein-analog fibers and characterize the fabricated fibers in terms of their morphological properties and *in vitro* degradation. The *in vitro* release kinetics were also studied together with the bioactivity of the released FGF9. The *in vitro* biocompatibility of the FGF9-loaded and unloaded electrospun fibers was tested using NIH-3T3, 10T1/2, and human coronary artery smooth muscle cells for potential therapeutic angiogenesis application.

MATERIALS AND METHODS

Materials

L-Phenylalanine, p-toluenesulfonic acid monohydrate, sebacoyl chloride, 1,4-butanediol and sodium carbonate (Alfa Aesar, Ward Hill, MA). Solvents, such as toluene, ethyl acetate, dimethyl sulfoxide (DMSO), chloroform ($CHCl_3$) and glass distilled dichloromethane (Caledon Laboratories, Georgetown, ON) were used without further purification. Bovine serum albumin was purchased from Sigma-Aldrich (Milwaukee, WI) and BCA protein assay kit from Thermo Scientific Pierce Inc. (IL, USA). Recombinant human fibroblast growth factor-9 (FGF9) and human FGF9 DuoSet ELISA kit were purchased from Cedarlane (Burlington, ON).

Synthesis of Poly(ester amide) by Interfacial Polymerization

The poly(ester amide) was prepared as previously reported (14). In the first step, di-p-toluenesulfonic acid salt monomer was prepared by acid-catalysed condensation. A suspension of L-phenylalanine (60.5 mM, 2.2 equivalents), p-toluenesulfonic acid monohydrate (66 mM, 2.4 equivalent), and 1,4-butanediol (27.5 mM, 1 equivalent) in toluene (100 mL) was heated to 140°C with stirring in a flask equipped with a Dean-Stark trap. The solution was heated at reflux for 48 h, and then the solvent was removed under vacuum. The resulting material was filtered and washed with toluene. The monomer was purified by dissolving in boiling deionized water (300 mL) followed by hot filtration, and the solution was left to recrystallize overnight at 4°C. The purification step

was repeated; afterwards, the monomer crystals were filtered and dried under vacuum.

In the second step, sebacoyl chloride (5 mM, 1 equivalent) was dissolved in glass distilled anhydrous dichloromethane (15 mL) and the solution was added drop-wise to an aqueous solution (15 mL) containing di-p-toluenesulfonic acid salt monomer (5.0 mM, 1 equivalent) and sodium carbonate (10 mM, 2 equivalents), and allowed to react for 12 h. Upon completion of the reaction, the solution was rotovapped. The polymer was then washed with deionized water prior to purification via Soxhlet extraction with ethyl acetate for 48 h followed by drying under vacuum.

Fabrication of PEA Electrospun Fibers

The electrospinning setup was equipped with a High Voltage DC Power Supply (ES30P, Gamma high voltage, USA), a glass syringe (Becton, Dickinson and Co., 0.5 cc, NJ, USA) with a blunt-tip stainless steel needle (conducting spinneret) controlled by a syringe pump (KD101, KD scientific, USA), and a static collector covered with aluminum foil. The process parameters including spinneret diameter (18–22 G) and applied voltage (15–20 kV), and the formulation parameters including polymer concentration (5.5–7%*w*/*w*) and solvent composition (Chloroform-to-dimethyl sulfoxide ratio) were optimized, in order to obtain bead-free fibers with uniform fiber diameter distribution.

Characterization of PEA Electrospun Fibers

Morphological analysis of the PEA fibers was performed using scanning electron microscopy (S-3400 N SEM, Hitachi, Japan). Electrospun fibrous mat samples were sputter-coated with gold/palladium (K550X sputter coater, Emitech Ltd., UK) and scanned at a working distance of 10 mm and a constant accelerating voltage of 20 kV. Three SE micrographs of the electrospun mats were analysed using computerised Image J software (NIH, Bethesda, MD, USA) to quantitatively determine mean fiber diameter from ten random measurements for each image. For transmission electron microscopy (Phillips CM10 TEM), the fibers were electrospun directly on the TEM grids for 30 s, and the samples were examined at 80 kV.

In Vitro Degradation Study

Samples of the fibrous mats (1×1 cm^2) were placed in a screw-capped glass vials filled with 10 mL of phosphate buffered saline (PBS 50 mM, pH 7.4) and removed at pre-determined time-points, rinsed with deionized water and vacuum dried for 48 h at room temperature for further analyses. Samples at the different degradation time-points were analysed morphologically using SEM. The weight loss was determined by the following equation: $\text{Mass loss} = \left[\frac{(Mi-Mt)}{Mi}\right] \times 100\%$, where, Mi is the initial dry weight of the fibrous mat at time 0 and Mt is the dry weight of the sample at the specific degradation time (after drying under vacuum). The molecular weights of the PEA fibers before and after degradation were determined using a Waters system gel permeation chromatography (GPC) equipped with two PLgel 5 μm (300×1.5 mm) columns at 85°C and connected to a PLgel guard column (Waters Ltd, Mississauga, ON). The eluent used was N,N-dimethylformamide (DMF) with 10 mM lithium bromide and 1% (*v*/*v*) triethylamine, and samples were injected (100 μL) at a flow rate of 1 mL/min and calibrated against polystyrene standards. Additional degradation studies were carried out in conditioned smooth muscle cell growth medium (CSmGM); human coronary artery smooth muscle cells were cultured in SmGM for 48 h, then the media was collected and used. Samples of 1×1 cm^2 fibrous mats were immersed in 1 mL of the degradation medium at 37°C, and the media were refreshed every week. Samples at different degradation time-points were removed, rinsed with deionized water, vacuum dried at room temperature and analyzed morphologically using SEM. To rule out the effect of the incubation temperature, dried PEA fiber mats were kept in a vial at 37°C as a control.

Loading PEA Fibers with Model Protein and Fibroblast Growth Factor-9

Bovine serum albumin (BSA) was incorporated into the PEA fibers using blend or emulsification electrospinning (5, 6). The electrospinning parameters was adopted from the previously conducted studies for plain fibers. Briefly, the PEA was dissolved in chloroform and dimethyl sulfoxide (DMSO) at a ratio of (9:1). The polymer solution (0.5 ml) was electrospun using a high voltage DC power supply set to 20 kV and a syringe with a blunt-tip stainless steel spinneret (22 gauge) kept at 8 cm from the grounded collector. The flow rate was kept at 0.1 mL/h using a syringe pump. In case of the blend electrospinning, BSA was dissolved in DMSO (1 μg/μL) and 100 μL were added to the polymer solution. While, for the emulsion electrospinning, 10 μL of stock BSA solution in PBS (10 μg/μL) were dropped and ultrasonicated in the polymer solution for 30 min in an ice bath. The same protocol was adopted for FGF9 loading, except for the lower initial loading (3 μg FGF9/0.5 mL polymer solution).

Determination of Percentage Entrapment Efficiency

Four milligrams of loaded PEA fibers were dissolved in 0.5 mL of chloroform and the tube was vortexed to dissolve the polymer. Afterwards, 2.5 mL of PBS (pH 7.4) were added

to extract the protein, and the system was centrifuged at 2,000 rpm for 5 min to separate the organic and aqueous phases. The aqueous phase was collected for BSA or FGF9 quantification using BCA protein assay kit (Thermo Scientific Pierce Inc., IL, USA) and ELISA assay kit (R&D systems, Inc., MN, USA), respectively. Three independent experiments on different PEA-loaded fiber batches each conducted in triplicate ($n=9$) were used to determine the percentage entrapment efficiency (% E.E.).

In Vitro Release Study of BSA and FGF9-Loaded PEA Electrospun Fibers

Samples of 1×1 cm^2 fibrous mats were placed in a 24-well plate, and incubated with 1 ml of phosphate-buffered saline (PBS 50 mM, pH 7.4) under continuous agitation (100 strokes/min), in a thermostatically controlled micro-plate shaker (VWR, USA) at 37°C. At pre-determined time intervals, the supernatant was collected and replenished with an equal volume of fresh buffer. The supernatants were immediately frozen at −80°C until further measurements. The amount of BSA released was quantified by BCA protein assay kit (Thermo Scientific Pierce Inc., IL, USA), while the amount of FGF9 released was quantified by ELISA assay kit (R&D systems, Inc., MN, USA). The absorbance was measured using a micro-plate reader (UVM 340, Montreal Biotech Inc., Canada) and the unknown concentration was determined from a pre-constructed calibration curve and the % E.E. data.

Bioactivity Assay of the Released Growth Factor

Bioactivity of the released growth factor from the electrospun scaffolds was assayed by *in vitro* evaluation of (NIH-3T3 cell line) mouse embryonic fibroblasts proliferation. NIH-3T3 cells were seeded in 96-well plates at a density of approximately 3,000 cells/well with 100 μL/well of advanced DMEM (GIBCO®, Invitrogen, Burlington, ON, Canada) containing 5% FBS, 1% antibiotics and 0.2 mM L-glutamine, in addition to 100 μL of the released FGF9 in PBS. After an incubation time of 48 h, cell metabolic activity was determined by MTT assay following the manufacturer's protocol (Vybrant®, Invitrogen, Burlington, ON, Canada). As a positive control, soluble FGF9 was added to the NIH-3T3 cells in amounts equivalent to those released from the FGF9-loaded scaffolds. The amount of added growth factor was calculated from the *in vitro* release data, combining release time points into: early-released FGF9 (from Day 1 to 13) and late-released FGF9 (from Day14 to 28) for both blend and emulsion electrospinning techniques. Cells cultured without FGF9 served as a negative control.

Cell Viability and Confocal Microscopy

Cell viability and metabolic activity on 2D PEA films (20 μL of 1%*w*/*v* PEA in DMF solvent casted), unloaded and FGF9-loaded 3D PEA electrospun scaffolds were quantified by MTT colorimetric assay. Circular samples (4 mm in diameter) of electrospun mats on aluminium foil were punched and affixed to a 96-well cell culture plate (BD Falcon™, Franklin Lakes, NJ) using silicone grease, sterilized by immersion in 70% ethanol (200 μL) for 30 min, and allowed to dry for one hour under germicidal UV light, before conditioning overnight in Hank's balanced salt solution (HBSS, 200 μL; Invitrogen Canada, Burlington, ON). NIH-3T3 cells were seeded onto samples at an initial cell density of approximately 3,000 cells/well and cultured for five days in advanced DMEM containing 5% FBS or serum-depleted conditions, and maintained in a humidified incubator at 37°C and 5% CO_2. At pre-determined time points, the medium was refreshed (100 μL), followed by the addition of 10 μL of 12 mM MTT solution to each well to make the final concentration 1.10 mM and then incubated at 37°C for 4 h. Yellow MTT salts are reduced to water-insoluble purple formazan by metabolically active cells. Afterwards, 100 μL 10% (*w*/*v*) SDS/HCl was added to solubilize the formazan, and further incubated at 37°C for 18 h. Finally, the coloured product was analyzed in 96-well plate and the absorbance was recorded at 570 nm by a micro-plate reader. Controls of TCPS were included in the experiments.

For confocal microscopy, NIH-3T3, 10T1/2, and HCASM cells were seeded, in 24-well plate at an initial cell density of approximately 2,000 cells/cm^2, on control glass coverslips, PEA films, FGF9-loaded PEA fibers, and PEA fibers with exogenous soluble FGF9, for three days. Cells were washed with pre-warmed PBS immediately prior to fixing at ambient temperature for 15 min in 4% formaldehyde solution (1 mL; EMD Chemicals) in divalent cation-free PBS. Following three washes in PBS, HCASMCs were permeabilized with 0.1% Triton X-100 (0.5 mL; VWR International, Mississauga, ON) in PBS for 5 min and again washed three times with PBS. The cells were incubated with 1% BSA in PBS (0.5 mL; Sigma-Aldrich, Oakville, ON) for 30 min at ambient temperature prior to their incubation with Alexa™ Fluor 568-conjugated phalloidin (1:50 dilution; Invitrogen Canada, Burlington, ON) in the dark for 1 h at ambient temperature followed by another three washes with PBS. The cells were then counterstained with 4′–6-diamidino-2-phenylindole dyhydrochloride (DAPI, 300 nM in PBS, 0.5 mL; Invitrogen Canada, Burlington, ON) for 5 min to label the nuclei and again washed three times with PBS. No.1 coverslips were mounted on microscope slides with Trevigen® Fluorescence Mounting Medium (Trevigen INC., Gaithersburg, MD). Samples were analyzed with a Zeiss LSM 5 Duo confocal microscope with nine laser lines and appropriate filters (Carl Zeiss, Toronto, ON, Canada).

RNA Isolation and Quantitative Real-time PCR Analysis

Real-time Polymerase Chain Reaction (qPCR) combined with reverse transcription was used to quantify messenger RNA (mRNA) expression of PDGFRβ in NIH-3T3 cells grown on control (TCPS), PEA fibers, FGF9-loaded PEA fibers, and PEA fibers with exogenous soluble FGF9, at a density of 2.5×10^5 cells/sample, for 24 h. Moreover, q-PCR was employed to study the effect of FGF9 concentration gradient on PDGFRβ gene expression in different cells (NIH-3T3, 10T1/2, and HCASMCs) grown on control (TCPS) and PEA fibers with exogenous soluble FGF9 of different concentrations (0, 8, 25, and 50 ng/mL). Total RNA from the cells was extracted using Trizol® reagent (Invitrogen, Burlington, Canada) following the manufacturer's protocol. Complementary DNA (cDNA) was synthesized using 1 μg of total RNA primed with oligo $(dT)_{12–18}$ as described in SuperScript™ (Invitrogen, Canada). Quantitative real-time PCR was conducted in 10 μl reaction volumes, using a CFX-96 Touch™ Real-time system C1000 Thermal Cycler (Bio-Rad, Mississauga, Canada) and gene expressions of mouse and human PDGFRβ were then determined with iQ™ SYBR® Green Supermix (Bio-Rad) according to the recommended protocol of the manufacturer. PDGFRβ forward primer: 5′-GGAGATTCGCAGGAGGTCAC-3′, reverse primer: 5′-ATAGCGTGGCTTCTTCTGCC-3′; GAPDH forward primer: 5′-GGTGGTCTCCTCTGACTTCAACA-3′, reverse primer: 5′-GTTGCTGTAGCCAAATTCGTTGT-3′. Amplification entailed 40 cycles of: denaturation 95°C (15 s), annealing 55°C (60 s), and extension 72°C (30 s). The relative mRNA expression in the cells was normalized to the housekeeping gene glyceraldehyde-3-phosphate dehydrogenase (GAPDH) with at least three repeats per experimental group and expressed as a relative ratio using the CFX Manager™ 3.0 analysis software (Bio-Rad, Mississauga, Canada).

Statistical Analysis

Data are presented as mean ± SEM for experiments conducted in triplicate. Statistical analysis was conducted with *t*-test or one-way ANOVA followed by Tukey's multiple comparison test using GraphPad Prism 4 software (GraphPad Software, Inc., CA, USA). Probability values less than 0.05 were considered statistically significant.

RESULTS AND DISCUSSION

Synthesis of PEA by Interfacial Polymerization

In this study, the PEA was synthesized by interfacial polymerization as previously reported and the results were consistent with previous data (14). The synthesized PEA, whose chemical structure is shown in Scheme 1 was designated as "8-Phe-4", whereby the 8 stands for the number of methylene groups contributed by the sebacic acid (diacid), the Phe is designated for L-phenylalanine (amino acid) and the 4 represents the number of methylene groups in the butanediol moiety (diol). The structure of 8-Phe-4 was confirmed through ^{1}H NMR. Interfacial polymerization is an irreversible condensation reaction occurring at the interface between two immiscible liquids; one of them is usually a water phase containing the di-functional monomer and inorganic base to activate the diol and neutralize the by-product acid, the other phase is an organic solvent containing the diacid chloride. Interfacial polymerization is preferred because it is rapid, less affected by impurities, and produces PEAs of higher molecular weights than solution polycondensation reactions (20).

Fabrication and Optimization of PEA Electrospun Fibers

PEA fibers were prepared using a solution electrospinning technique. Our goal was to develop bead-free fibers from high molecular weight-PEA and optimize the electrospinning parameters to obtain fibers of average fiber diameter between 100–500 nm, in order to mimic the extracellular matrix fiber diameter. It is clear from the electrospinning processes literature that the structure and morphology of the produced fibers are determined by a synergetic effect of formulation and process parameters. Formulation parameters including the effect of polymer concentration and solvent composition on fiber morphology were studied. Increasing the polymer concentration in 100% chloroform ($CHCl_3$) from 5.5 to7% *w*/*w*, electrospun at 8 cm/20 kV, 22 G, and 0.1 mL/h flow rate resulted in increasing the average fiber diameter from 445 to 655 nm as illustrated in Fig. 1. This also led to decreased bead formation, where they transformed from spherical-shaped beads to spindle-like beads to bead-free fibers. This is consistent with previous data reporting that increasing the polymer solution viscosity by increasing its polymer concentration yielded uniform fibers with fewer beads and junctions (21). However, at polymer concentration of 7% *w*/*w*, the polymer solution was too viscous, and chloroform evaporated too fast (B.P.=61°C), which resulted in drying out of the polymer at the needle tip. This phenomenon was previously reported for concentrated solutions (and therefore

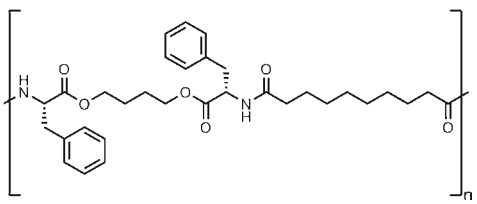

Scheme 1 Chemical structure of 8-Phe-4

too viscous) (22), which in our study interrupted the electrospinning process several times, demanding for an alternative solvent system.

Regarding the effect of solvent composition and conductivity on the fiber morphology, the use of a binary solvent system of chloroform and dimethylsulfoxide, $CHCl_3$/DMSO (9:1), instead of 100% $CHCl_3$ resulted in eliminating the beads as illustrated in Fig. 1(d-f). This can be attributed to the high dielectric constant of DMSO ($\varepsilon = 46.6$) contributing to the increased conductivity of the polymer solution. It has been shown that increasing the polymer solution conductivity can be used to produce more uniform fibers with fewer beads, and solvents that had sufficiently high values of dielectric constant were found to be used successfully in electrospinning (21, 23). Further increase in the DMSO concentration resulted in fiber fusion, due to residual DMSO that could not evaporate (B.P. = 189°C) from the polymer solution before the fibers hit the grounded collector.

Processing parameters such as the applied voltage and spinneret diameter were also studied. Figure 2 illustrates the effect of the applied voltage on fiber morphology and diameter. In the case of single solvent system of $CHCl_3$, reducing the applied voltage from 20 to 15 kV resulted in decreased fiber diameter from 380 to 255 nm; however, it did not affect the fiber morphology. It has been shown that increased voltages produces jets with larger diameters and ultimately leads to the formation of several jets and the presence of beads in many polymeric systems (21). In regards to the effect of spinneret diameter, 6% *w*/*w* PEA in $CHCl_3$/DMSO (9:1) was electrospun at 20 kV, 8 cm, and 0.1 mL/h flow rate with increasing needle gauge from 18 to 22 gauge, which corresponds to decreasing the spinneret diameter. This resulted in a reduction in the mean fiber diameter from 345 to 250 nm and more uniform fiber diameter distribution as shown in Fig. 2 (d-f). Based on the optimization of PEA electrospun fibers data, the elelectrospinning parameters were fixed at 6% *w*/*w* PEA in $CHCl_3$/DMSO (9:1), electrospun at 20 kV, 8 cm, 22 guage needle, and 0.1 mL/h flow rate in all subsequent experiments.

In Vitro Degradation Study

Scaffold degradation in phosphate buffered saline (pH 7.4) at 37°C for a period up to four weeks was examined qualitatively using scanning electron microscopy and quantitatively by mass loss determination and molecular weight analysis using GPC. The effect of temperature alone during the degradation of the fibers was excluded by incubating control dry fiber mats at 37°C inside a glass vial. Since the glass transition temperature of 8-Phe-4 is 41°C, we did not anticipate observable changes on the fiber morphology such as fiber flattening and subsequent fusion over the 28 days (top panel in Fig. 3a). Scanning electron (SE) micrographs showed that scaffolds incubated in PBS preserved their fibrous structure over the four-week study period, with negligible morphological changes when compared to the control at 37°C (middle panel in

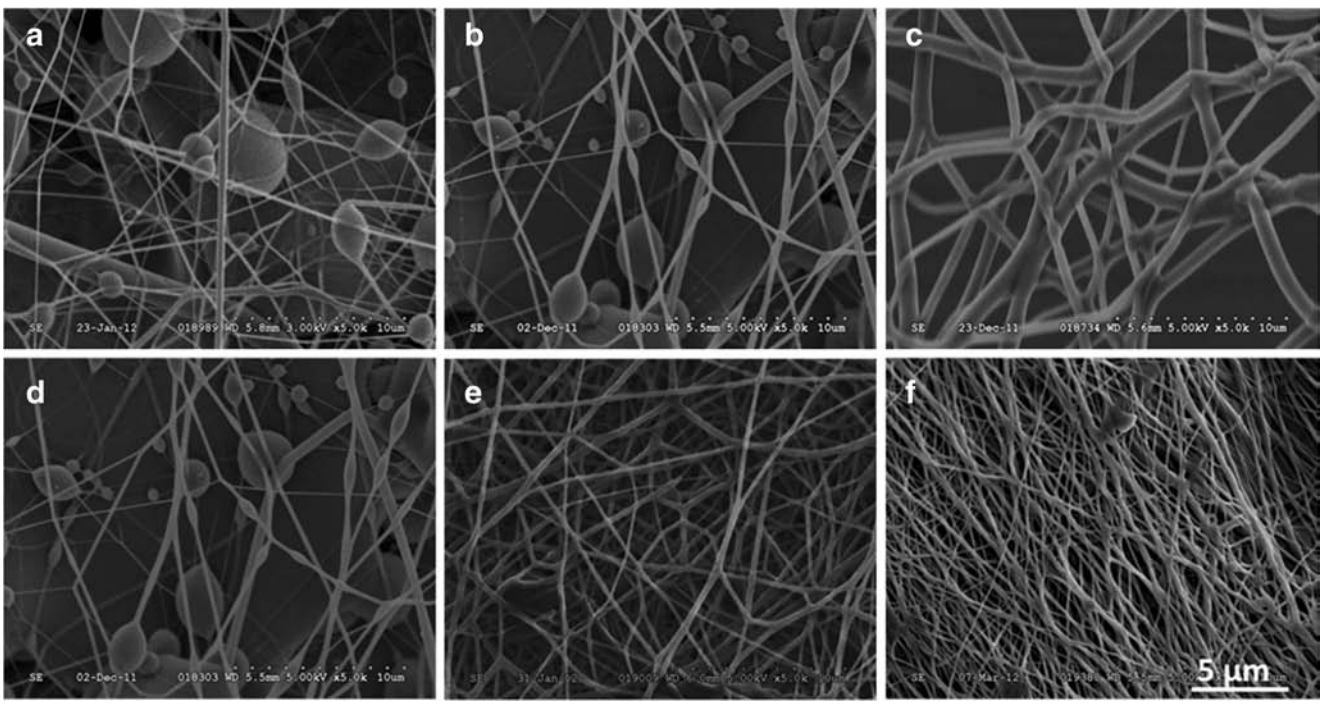

Fig. 1 Optimization of formulation electrospinning parameters: Effect of polymer concentration on fiber morphology and fiber diameter, 8-Phe-4 in $CHCl_3$ (**a**) 5.5% *w*/*w*, (**b**) 6% *w*/*w*, and (**c**) 7% *w*/*w*. Effect of solvent composition on fiber morphology and diameter, 6% *w*/*w* 8-Phe-4 in $CHCl_3$/DMSO ratio of (**d**) (10:0), (**e**) (9:1), and (**f**) (8:2), electrospun at 8 cm/20 kV, 22 G, and 0.1 mL/h flow rate.

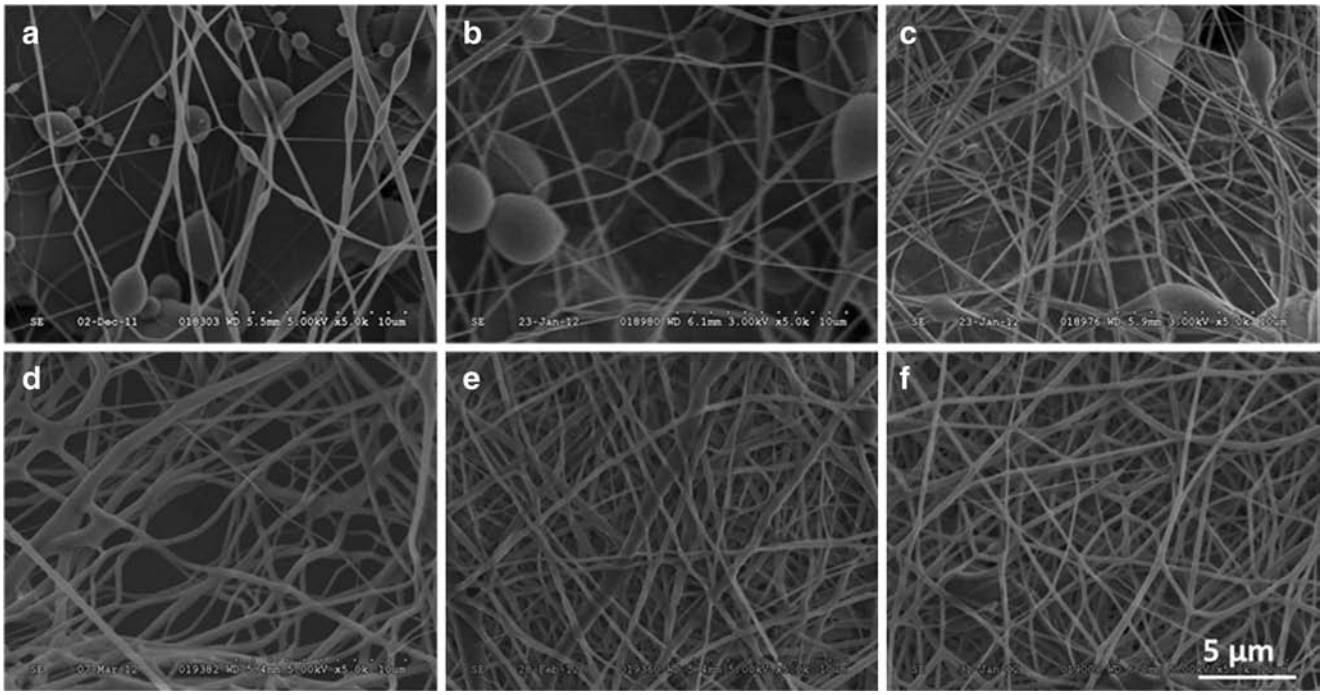

Fig. 2 Optimization of process electrospinning parameters: Effect of applied voltage on fiber morphology and diameter, electrospun fibers of 6% *w/w* 8-Phe-4 in $CHCl_3$ at (**a**) 20 kV, (**b**) 17 kV, and (**c**) 15 kV. Effect of spinneret diameter on fiber morphology and diameter, 6% *w/w* 8-Phe-4 in $CHCl_3$/DMSO (9:1) was electrospun from (**d**) 18 gauge, (**e**) 20 gauge, and (**f**) 22 gauge needle.

Fig. 3a). Moreover, quantitative analysis showed 21% mass loss over the 28 day study period together with insignificant change in average number molecular weight (M_n) over the four weeks (Figs. 3b and c). The degradation study was terminated after 28 days since our goal for developing the controlled release system is to replace the osmotic infusion pump as means of FGF9-delivery employed in our previous work for therapeutic angiogenesis (12). The linear decrease in mass ($r^2=0.97$), coupled with constant molecular weight indicate that the PEA scaffold degradation is dominated by surface erosion (18, 24). The polydispersity indices of the samples during the incubation time in PBS for four weeks were 2.88 $\pm$0.15, further supporting the absence of bulk degradation. Additionally, we have studied the effect of biorelevant media on the degradation of the PEA fibers, so additional degradation studies were carried out in a conditioned smooth muscle cell growth medium (CSmGM); human coronary artery smooth muscle cells (HCASMCs) were cultured in SmGM for 48 h, in which the HCASMCs would have consumed the nutrients necessary for their growth and secreted their metabolites and other products relevant to growth in culture, then the media was collected and used for the degradation study. The SE micrographs showed that the fibers did withstand this biorelevant medium with some fiber swelling and fusion starting from Week 3 (bottom panel in Fig. 3a). The *in vitro* degradation data suggests that surface eroding PEA electrospun fibers can be employed for controlled delivery of bioactive molecules in biorelevant conditions.

In Vitro Release Study of Loaded PEA Electrospun Fibers

The model protein, bovine serum albumin (100 μg BSA/cm^2), was successfully loaded into the PEA fibers using blend or emulsification electrospinning (5, 6). The percentage entrapment efficiency (% E.E.) for blend and emulsion electrospun BSA-loaded fibers was 93%$\pm$3 and 73%$\pm$4, respectively. The lower entrapment efficiency for the emulsion electrospun fibers is related to the relatively higher viscosity of the emulsified protein/polymer mixture compared to the blend where the protein was dissolved. Transferring a more viscous emulsion from an emulsification vial to an electrospinning syringe causes some material loss. The residual protein/polymer solution left on the inner wall of the syringe after electrospinning also accounts for some material loss.

Samples of 1×1 cm^2 fibrous mats were placed in a 24-well plate, and incubated with 1 ml of phosphate-buffered saline (PBS 50 mM, pH 7.4) under continuous agitation (100 strokes/min) at 37°C. At predetermined time intervals, the amount of BSA released was quantified by BCA protein assay kit. BSA release was sustained over the 28 day study with a limited burst effect and 80% BSA liberation from the blend electrospun BSA-loaded PEA fibers (Fig. 4a). Given that the mass loss during the 28 days is 21%, the higher BSA release is related to its higher initial protein loading. Incorporation of higher amounts of a protein into the fibers is believed to be a

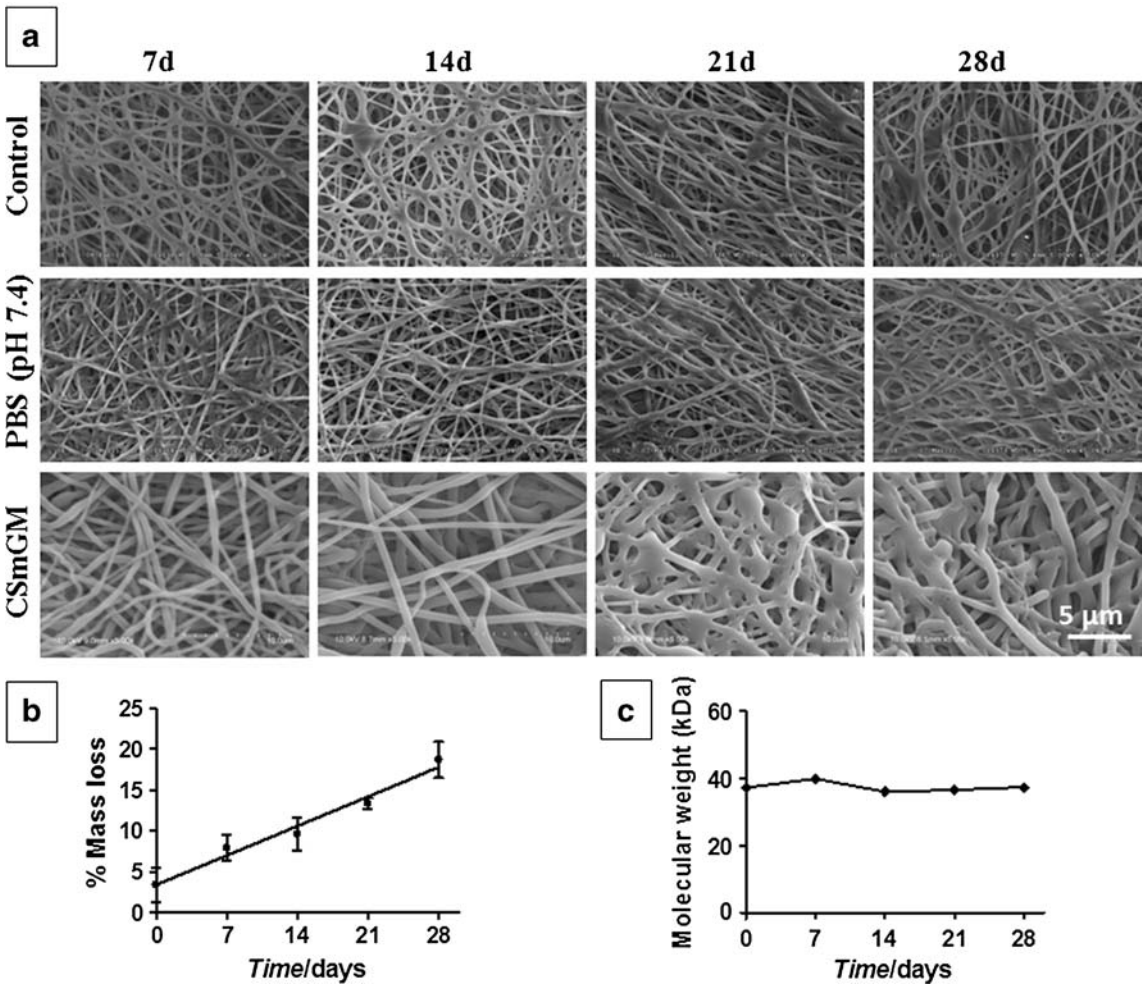

Fig. 3 *In vitro* degradation of PEA electrospun fibers at 37°C for 28 days. (**a**) SE micrographs for fibers in PBS (pH = 7.4) and conditioned human smooth muscle cell growth medium, the control is dry PEA fibers kept at 37°C. (**b**) Percentage mass loss of PEA fibers in PBS (pH = 7.4) at 37°C at different time points ($n = 3$) and (**c**) molecular weight analysis using gel permeation chromatography.

driving force for protein molecules to migrate toward the surface of the fiber during electrospinning (25). The absence of burst release highlighted BSA uniform entrapment with the polymer solution (26), resulting in perfect inclusion within the fibers (27), while the sustained release pattern confirmed the adequate structural integrity of the fibers throughout the study. For emulsion electrospun fibers, the release profile showed a decreased BSA release rate in comparison with blend electrospun fibers, reaching 37% at Day 28. This is predictable based on the notion that BSA is encapsulated in the aqueous vesicles (as demonstrated in Fig. 4c), which can be referred to as a "diffusion-across-a-barrier type release system" (16); this requires the degradation of the polymeric matrix, then subsequent diffusion of BSA from the vesicles across the outer barrier layer. During an emulsion electrospinning process, the emulsion droplets move from the surface to the center to achieve their highest accumulation along the axial region (6, 28). This inward migration of emulsion droplets is caused by rapid evaporation of the solvents during electrospinning. As the organic solvent evaporates faster than water, the viscosity of the outer layer of a fiber increases more rapidly than that of its inner layer resulting in a viscosity gradient between the aqueous droplets and the polymer matrix, which directs the emulsion droplets to settle into the fiber core rather than on the surface (16, 29).

BSA-loaded PEA fibers prepared by both electrospinning techniques followed a time-dependent power law function: $\frac{\mathbf{Mt}}{\mathbf{M}\infty} = \mathbf{k}\,\mathbf{t}^{\mathbf{n}}$, where, $\frac{\mathbf{Mt}}{\mathbf{M}\infty}$ is the fractional release, k is a structural/geometric constant, t is the time and n is the release exponent representing the release mechanism. The n values of blend and emulsion electrospun BSA-loaded fibers were 0.62 and 0.58, respectively. For cylindrical constructs (for which the individual fiber can be modelled), an n value between 0.45 and 0.89 indicates a coupled matrix degradation and biomolecule diffusion release mechanism (30).

Following the proof-of-concept of incorporating a model protein into PEA electrospun fibers, FGF9 was loaded into the PEA fibers adopting both electrospinning techniques. The % E.E. of FGF9 was 86% ±3 and 80% ±3 for blend and

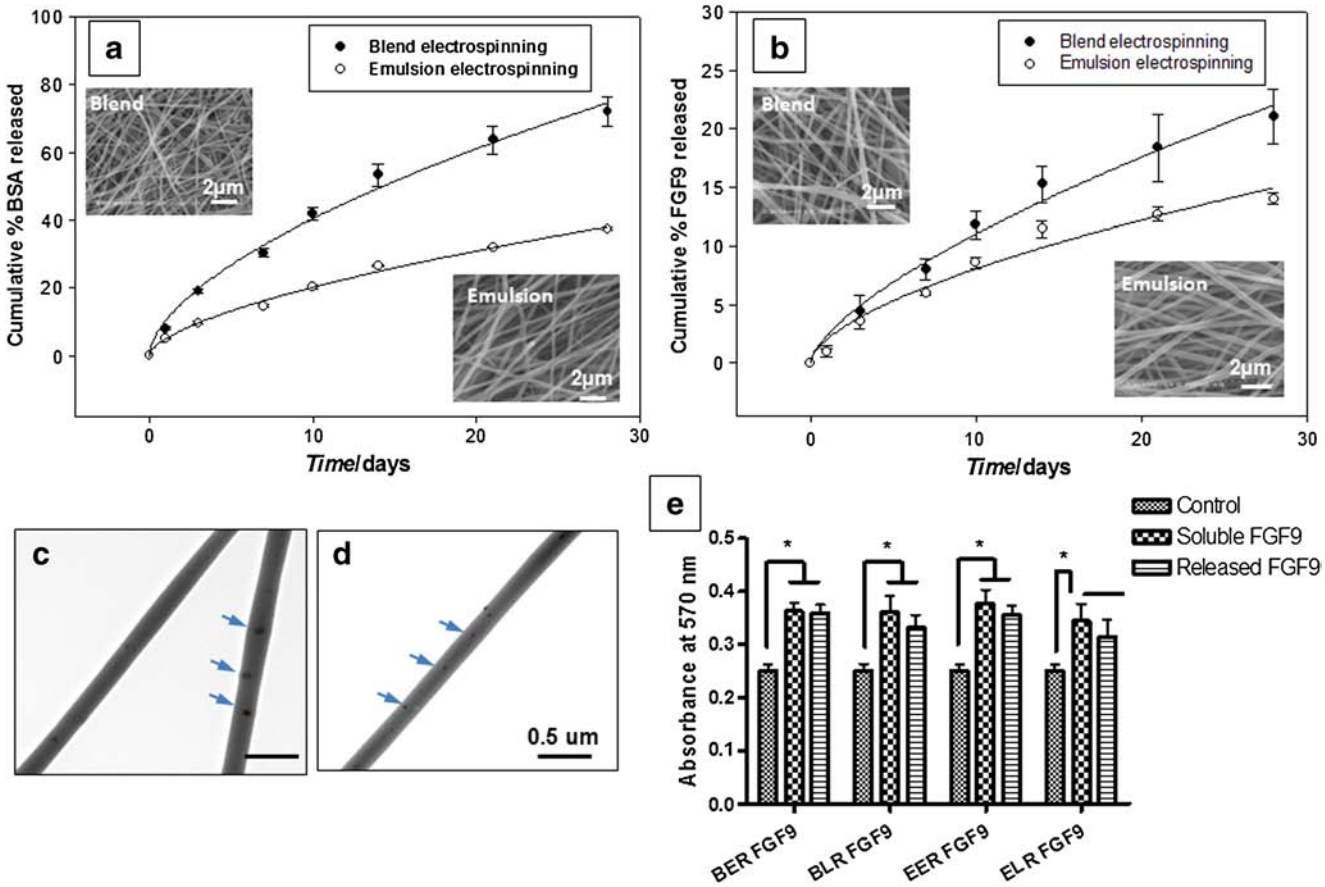

Fig. 4 *In vitro* release study of (**a**) BSA-loaded PEA fibers and (**b**) FGF9-loaded PEA fibers, using blend and emulsion electrospinning techniques, in PBS (pH = 7.4) at 37°C ($n = 3$). (**c**) TEM of BSA-loaded PEA fibers and (**d**) TEM of FGF9-loaded PEA fibers, using the emulsion electrospinning technique (arrows are pointing to the aqueous vesicles). (**e**) Bioactivity study of FGF9 released from FGF9-loaded PEA fibers using MTT assay. Two-release time points were tested; early-released FGF9 (from Day 1 to Day 13) and late-released FGF9 (from Day 14 to Day28) for blend and emulsion techniques. Positive controls of soluble FGF9 were included in the experiment. Data represents mean ± SEM from three independent experiments (*$p < 0.05$).

emulsion electrospun FGF9-loaded fibers, respectively, using ELISA kit. FGF9-loaded fibers showed a similar release profile (Fig. 4b) with a significant decrease in the overall release rate, due to the lower initial protein loading (~120 ng/cm^2). Similarly, the release exponent for blend and emulsion electrospun FGF9-loaded fibers was 0.67 and 0.59, respectively, indicating also a non-Fickian diffusion mechanism. Although our ultimate goal is to deliver FGF9 *in vivo*, BSA release studies were also conducted in this work. The rationale for using BSA was two-fold: i) it is a widely studied model protein in controlled-release studies and, ii) it is a large protein (66.5 kDa) compared with FGF-9 (23 kDa) allowing us to study the capability of PEA fibers to release proteins of different sizes in a similar mechanism. Our data (Figs. 4a and b) showed the release mechanism for both proteins was the same suggesting that PEA electrospun fibers had shown versatility for loading different bioactive molecules (BSA and FGF9). The ability to introduce bioactive molecules into these fibrous electrospun meshes, through these aqueous pouches opens a new path to therapeutic agent delivery.

Bioactivity Assay of the Released Growth Factor

A cell proliferation-based assay was used to assess the bioactivity of FGF9 released at early (Day 1-Day 13) and late (Day 14-Day 28) collective time points from the PEA electrospun fibers using blend and emulsion techniques. The proliferating cell number was determined by a 3–(4,5-dimethylthiazol-2-yl)-2,5-diphenyltetrazolium bromide (MTT) assay on NIH-3T3 fibroblasts incubated for 48 h with media containing released FGF9 or equivalent amounts of soluble FGF9 calculated from the *in vitro* release data (positive control). There was no significant difference ($p < 0.05$) in metabolic activity between the released and control FGF9 (Fig. 4e). These results indicate that FGF9 released from the fibers, prepared either by blend or emulsion techniques, was bioactive up to 28 days. It is worth noting that the emulsion late-released (ELR) time point did not show a significant difference from the untreated control (no FGF9 added), which can be attributed to the lower released amount of FGF9 in case of ELR in comparison with the other three tested conditions.

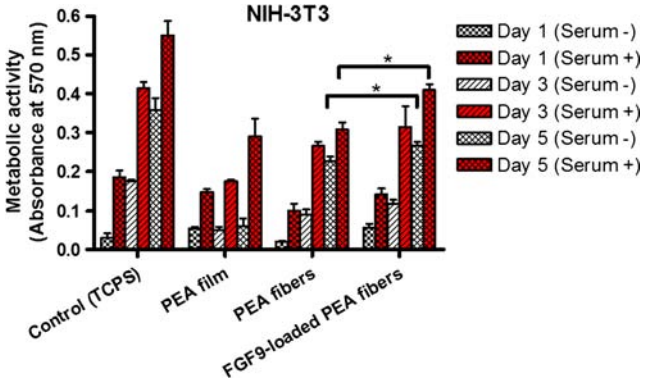

Fig. 5 NIH-3T3 cell viability study on 2D PEA films (1%*w/v*), unloaded and FGF9-loaded 3D PEA emulsion electrospun fibers for 5 days, in Serum + (5% FBS) and Serum − (serum depleted) conditions, using MTT assay. Data represents mean ± SEM from three independent experiments (*$p < 0.05$).

Cell Viability and Confocal Microscopy

For evaluation of the PEA electrospun fibers *in vitro* biocompatibility as potential drug delivery vehicle for bioactive molecules, cell viability on FGF9-loaded 3D fibers was assessed using the MTT assay and compared to 2D PEA films and unloaded 3D fibers. For this section and the following one, FGF9-loaded PEA fibers prepared by emulsion electrospinning instead of blend electrospinning were used for two reasons: (i) we wanted to provide a maximum protection for FGF9 from the organic solvent (i.e. chloroform) during electrospinning, (ii) our long-term goal is to use the fibers as a dual growth factor delivery system (the first one for inducing angiogenic sprout formation and the second one to recruit mural cells for neovessel maturation and functionality after the formation of the endothelial tubes). Since FGF9 release is needed for neovessel maturation, its delayed release is beneficial.

As shown in Fig. 5, 2D PEA films, and both FGF9-loaded and unloaded fibers supported fibroblast proliferation for up to five days, in the case of 5% FBS (Serum+) conditions. In the case of serum-depleted (Serum−) conditions, the unloaded and FGF9-loaded 3D PEA fibers maintained cell growth and proliferation through the five-day study, whereas 2D

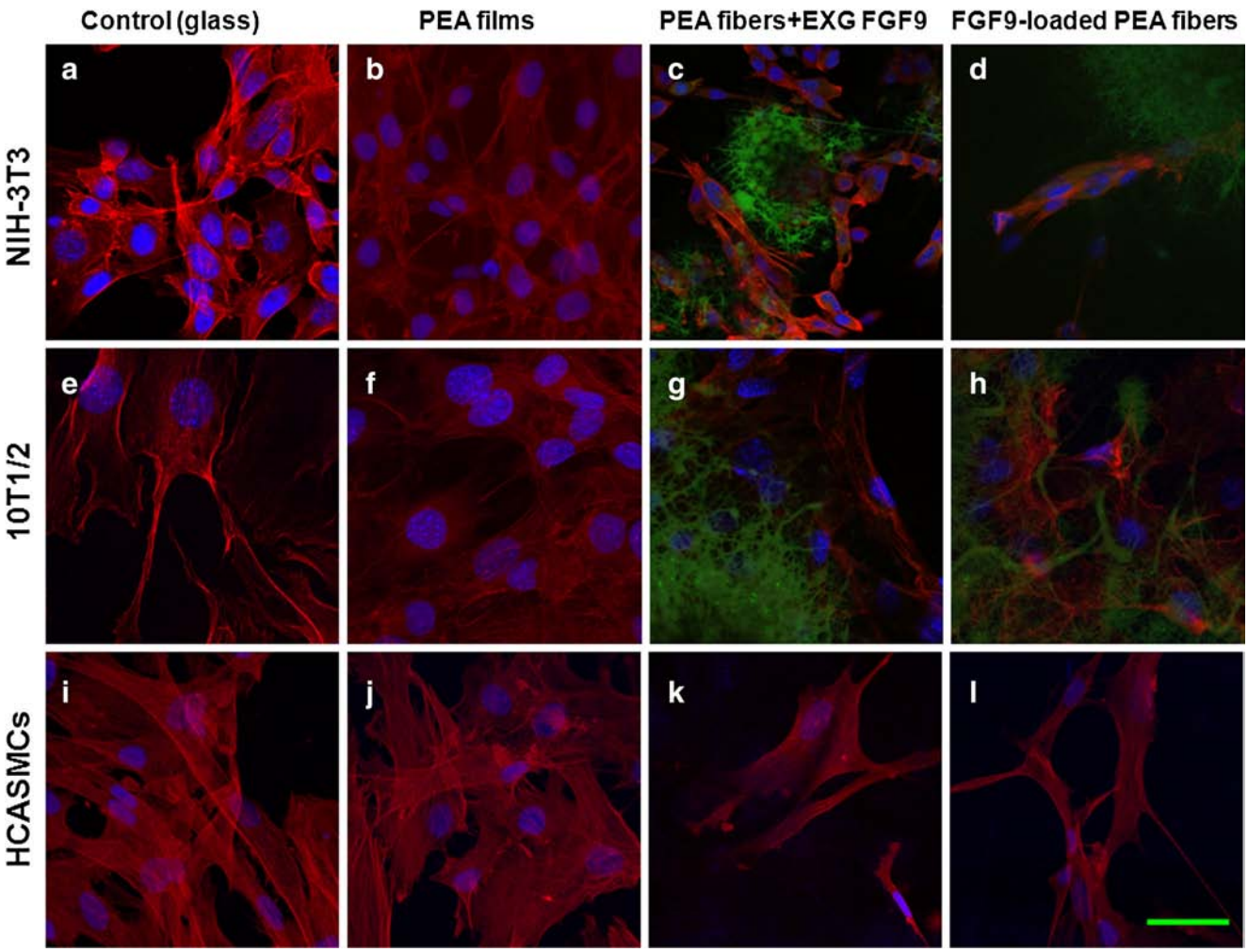

Fig. 6 Confocal microscopy images of NIH-3T3, 10T1/2, and HCASMCs seeded at 2,000 cells/cm^2 for 3 days on glass coverslips (control), PEA films, PEA fibers with exogenous FGF9, and FGF9-loaded PEA emulsion electrospun fibers, showing F-actin (red), nuclei (blue), and fibers (green). Scale bar = 40 μm.

PEA films supported only the survival of cells. Baker and Southgate (31) attempted to culture stromal cells on 3D polystyrene fibers in serum-depleted conditions, but stromal cells failed to adhere to the polystyrene fibrous scaffold in the absence of serum; in contrary to this our PEA electrospun fibers were able to support the attachment and proliferation of fibroblasts in serum-depleted conditions, which could be attributed to potential peptide linkages imparted by the amino acid-based PEA fibers.

To further assess the PEA electrospun fibers as a potential sustained-delivery vehicle for FGF9, we have examined their interactions with different cell types (NIH-3T3, 10T1/2, and HCASMCs) using confocal microscopy. FGF9 has reported proliferative effect on 3T3 (32, 33) and smooth muscle cells (10, 12). As for 10T1/2 cell line, it is a smooth muscle precursor cell type that is commonly used for *in vitro* SMC phenotype studies because of its ability to maintain a stable phenotype in culture and even can be pushed toward an SMC state (34). The cells showed good attachment and spreading on glass control and 2D PEA surfaces, and displayed interaction and infiltration in case of the 3D PEA electrospun fibers either FGF9-loaded or with exogenous supplementation of FGF9 as shown in Fig. 6. The PEA fibers had inherent autofluorescence in the green channel, which was obscured in case of HCASMCs (Figs. 6k and l) due to the use of different culture medium (Medium 231 supplemented with SMGS, GIBCO®, Invitrogen, Burlington, ON, Canada). Biodegradable PEAs have been previously reported to support attachment, spreading, and proliferation of human coronary artery smooth muscle cells, bovine aortic endothelial cells, and fibroblasts (14, 18, 35, 36). Together with the fact that 3D scaffolds play an important role in guiding cells to produce their own extracellular matrix and control phenotype differentiation (37, 38), by providing both mechanical and biological cues, PEA electrospun fibers were found to support cell growth even in serum-depleted conditions. These data highlight the potential expanding applications of PEA fibers in drug delivery and tissue engineering.

RNA Isolation and Quantitative Real-Time PCR Analysis

To understand the signaling pathways underlying the reported FGF9-induced investment of neovessels by SMCs, we

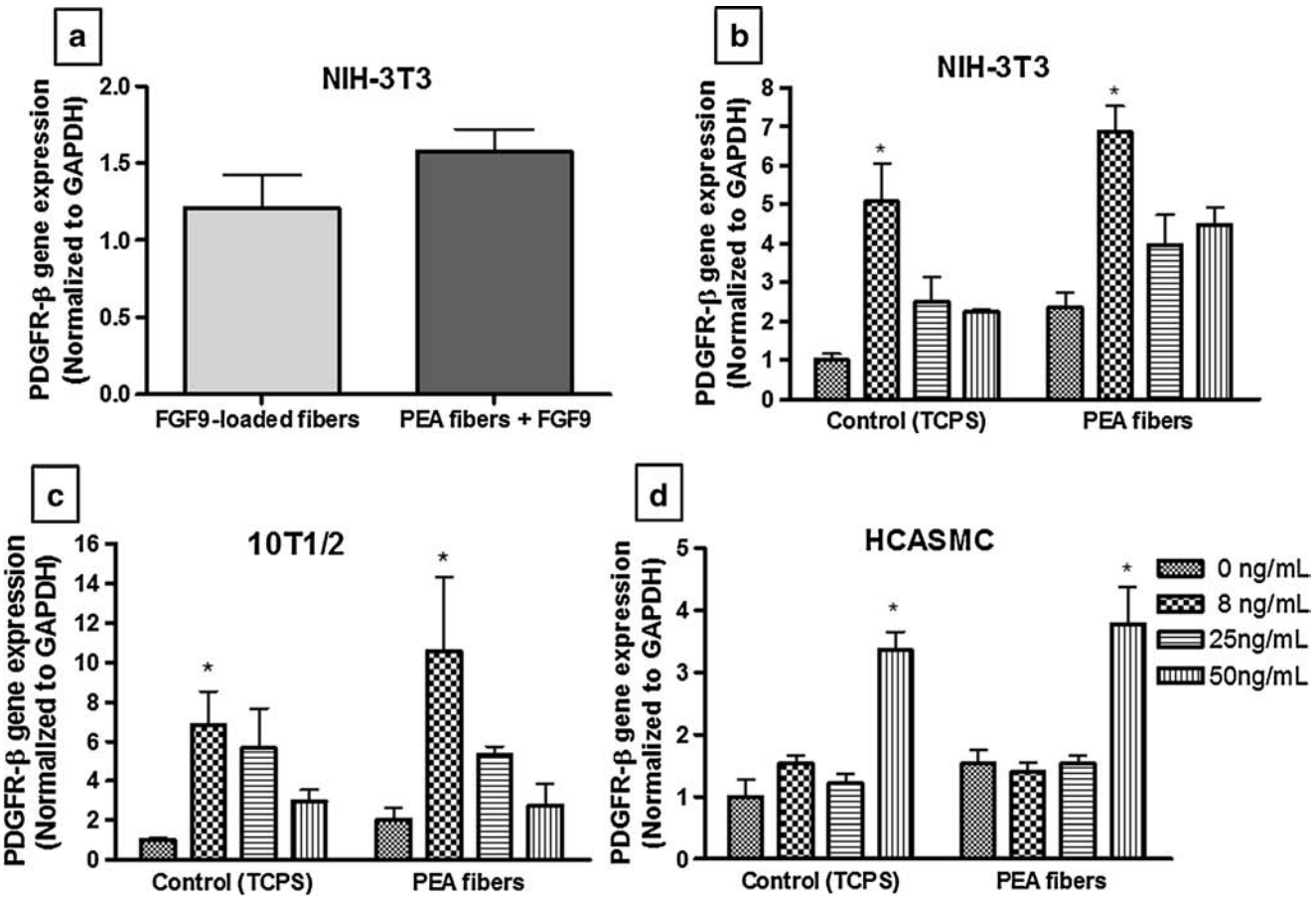

Fig. 7 (**a**) Quantitative real-time PCR analysis of PDGFR-ß expression for NIH-3T3 cells seeded on FGF9-loaded emulsion electrospun fibers and PEA fibers with exogenous FGF9 for 24 h. (**b**) Effect of FGF9 concentration gradient on PDGFR-ß gene expression in NIH-3T3, 10T1/2, and HCASMC cells, seeded on TCPS (control) and PEA fibers with exogenous FGF9 for 24 h. Data represents mean ± SEM and values of $p < 0.05$ were considered statistically significant ($n = 3$).

studied the expression of platelet-derived growth factor receptor-β (PDGFRβ), which is one of the downstream signaling molecules in FGF9-stimulated SMCs. PDGFRβ is a well-documented regulator of SMC migration (39) and therefore a potential mediator of FGF9-induced vessel maturation. Real-time Polymerase Chain Reaction (qPCR) preceded with reverse transcription was used to quantify messenger RNA (mRNA) expression of PDGFRβ in NIH-3T3 cells grown on control (TCPS), PEA fibers, FGF9-loaded PEA fibers, and PEA fibers with exogenous soluble FGF9, at a density of 2.5×10^5 cells/sample, for 24 h. q-PCR analysis of PDGFRβ expression showed insignificant difference between NIH-3T3 cells seeded on PEA fibers, FGF9-loaded fibers, or PEA fibers with exogenous FGF9 (~8 ng/mL, equivalent to the amount released from the FGF9-loaded PEA fibers after 24 h) as illustrated in Fig. 7a, suggesting that the FGF9 exogenously supplemented to PEA fibers is equivalent to the released FGF9 from the loaded PEA fibers. Thus, the FGF9 exogenously supplemented PEA fibers were selected to map the effective FGF9 concentration required for PDGFRβ upregulation, for future loading into the PEA fibers. Consequently, the effect of FGF9 concentration on PDGFRβ gene expression was further studied in different cells (NIH-3T3, 10T1/2, and HCASMCs) seeded on control (TCPS) and PEA fibers with exogenous soluble FGF9 of different concentrations (0, 8, 25 and 50 ng/mL). The q-PCR data showed significant upregulation in the PDGFRβ expression at the lowest tested FGF9 concentration (8 ng/mL) for NIH-3T3 and 10T1/2 cells (Figs. 7b and c). In contrast, the highest tested FGF9 concentration (50 ng/mL) was the concentration that resulted in significant upregulation in the case of HCASMCs (Fig. 7d). Recent studies have shown that pre-treatment of SMCs with FGF9 (100 ng/ml) for 24 h was found to increase their chemotactic response to PDGF-BB (40), which is a ligand for PDGFRβ and a growth factor necessary for mural cell recruitment during development and can promote vascular stability (41). As well, there was substantial increase in PDGFRβ expression in SMC pre-exposed to increasing concentrations of FGF9 (10–100 ng/mL) (12). Furthermore, when a PDGFRβ blocking antibody was added to angiogenic implants, it did not affect their vascularity after 2 weeks but reduced the number of vessels invested by mural cells expressing smooth muscle α-actin (12). The current findings support the premise that FGF9 is a regulator of PDGFRβ expression, which is the receptor necessary for FGF9-induced mural cell recruitment, and that the critical concentration of FGF9 varies between mouse fibroblasts, 10T1/2 cells, and human smooth muscle cells. This study may provide important platforms for therapeutic angiogenesis and tissue engineering applications.

CONCLUSIONS

Biodegradable poly(ester amide) fibers were successfully fabricated using electrospinning techniques. Bead-free fibers of mean fiber diameter ~250 nm and uniform fiber diameter distribution were produced using a binary solvent system of chloroform and DMSO (9:1). PEA electrospun fibers preserved their fibrous structure over the four-week *in vitro* degradation study in PBS (pH 7.4) and conditioned smooth muscle cell growth medium at 37°C. Loaded PEA fibers exhibited controlled-release of BSA and FGF9 over 28 days with a limited burst effect for both blend and emulsion electrospun fibers and preserved FGF9 bioactivity. Moreover, the FGF9-loaded PEA elecrospun fibers were found to maintain the growth and proliferation of mouse fibroblasts for up to five days. Finally, q-PCR analysis suggests that FGF9 is a stimulator of PDGFRβ expression, which is the receptor necessary for FGF9-induced mural cell recruitment and vessel maturation. These data support the premise of FGF9 sustained delivery from PEA electrospun fibers and its potential application in therapeutic angiogenesis and regenerative medicine. Future work is required to examine dual loading of angiogenic growth factors and evaluating the induced angiogenesis *in vitro* and *in vivo*.

ACKNOWLEDGMENTS AND DISCLOSURES

The Authors acknowledge the financial support from The Heart and Stroke Foundation of Canada (T-7262), the Natural Sciences and Engineering Research Council of Canada, the Canadian Institutes for Health Research (FRN 11715), and the Canadian Cancer Society (Grant #701080). S. S. Said held a CIHR Strategic Training Fellowship in Vascular Research (2011–2013). J. G. Pickering holds the Heart and Stroke Foundation of Ontario/Barnett-Ivey Chair. Thanks to D. K. Knight for his assistance in the synthesis of PEA and performing the GPC molecular weight analysis.

REFERENCES

1. Dragneva G, Korpisalo P, Yla-Herttuala S. Promoting Blood Vessel Growth in Ischemic Diseases: Challenges in Translating Preclinical Potential into Clinical Success. Dis Model Mech. 2013;6(2):312–22.
2. Lusis AJ. Atherosclerosis. Nature. 2000;407(6801):233–41.
3. Lee KY, Peters MC, Mooney DJ. Comparison of Vascular Endothelial Growth Factor and Basic Fibroblast Growth Factor on Angiogenesis in SCID Mice. J Control Release. 2003;87(1–3):49–56.
4. Said SS, Pickering JG, Mequanint K. Advances in Growth Factor Delivery for Therapeutic Angiogenesis. J Vasc Res. 2013;50(1):35–51.
5. Sahoo S, Ang LT, Goh JC-H, Toh SL. Growth Factor Delivery Through Electrospun Nanofibers in Scaffolds for Tissue Engineering Applications. J Biomed Mater Res. 2010;93A:1539–50.

6. Yang Y, Xia T, Zhi W, Wei L, Weng J, Zhang C, *et al.* Promotion of Skin Regeneration in Diabetic Rats by Electrospun Core-Sheath Fibers Loaded With Basic Fibroblast Growth Factor. Biomaterials. 2011;32(18):4243–54.
7. Seyednejad H, Ji W, Yang F, van Nostrum CF, Vermonden T, van den Beucken JJ, *et al.* Coaxially Electrospun Scaffolds Based on Hydroxyl-Functionalized Poly (Epsilon-Caprolactone) and Loaded With VEGF for Tissue Engineering Applications. Biomacromolecules. 2012;13(11):3650–60.
8. Roy RS, Roy B, Sengupta S. Emerging Technologies for Enabling Proangiogenic Therapy. Nanotechnology. 2011;22(49):494004.
9. Rubanyi GM. Angiogenesis in health and disease: Basic mechanisms and clinical applications. New york: Marcel Dekker Inc.; 2000.
10. Agrotis A, Kanellakis P, Kostolias G, Di Vitto G, Wei C, Hannan R, *et al.* Proliferation of Neointimal Smooth Muscle Cells After Arterial Injury. Dependence on Interactions Between Fibroblast Growth Factor Receptor-2 and Fibroblast Growth Factor-9. J Biol Chem. 2004;279(40):42221–9.
11. Spicer D. FGF9 on the Move. Nat Genet. 2009;41(3):272–3.
12. Frontini MJ, Nong Z, Gros R, Drangova M, O'Neil C, Rahman MN, *et al.* Fibroblast Growth Factor 9 Delivery During Angiogenesis Produces Durable, Vasoresponsive Microvessels Wrapped by Smooth Muscle Cells. Nat Biotechnol. 2011;29(5):421–7.
13. Richardson TP, Peters MC, Ennett AB, Mooney DJ. Polymeric System for Dual Growth Factor Delivery. Nat Biotechnol. 2001;19(11):1029–34.
14. Knight DK, Gillies ER, Mequanint K. Strategies in Functional Poly (ester amide) Syntheses to Study Human Coronary Artery Smooth Muscle Cell Interactions. Biomacromolecules. 2011;12(7):2475–87.
15. Vert M, Li S, Garreau H. New Insights on the Degradation of Bioresorbable Polymeric Devices Based on Lactic and Glycolic Acids. Clin Mater. 1992;10(1–2):3–8.
16. Szentivanyi A, Chakradeo T, Zernetsch H, Glasmacher B. Electrospun Cellular Microenvironments: Understanding Controlled Release and Scaffold Structure. Adv Drug Delivery Rev. 2011;63(4–5):209–20.
17. Li L, Chu CC. Nitroxyl Radical Incorporated Electrospun Biodegradable Poly (Ester Amide) Nanofiber Membranes. J Biomater Sci Polym Ed. 2009;20(3):341–61.
18. Srinath D, Lin S, Knight DK, Rizkalla AS, Mequanint K. Fibrous Biodegradable L-alanine-based Scaffolds for Vascular Tissue Engineering. J Tissue Eng Regen Med. 2012.
19. Valle L, Roa M, Diaz A, Casas M, Puiggali J, Rodriguez-Galan A. Electrospun Nanofibers of a Degradable Poly (Ester amide). Scaffolds Loaded with Antimicrobial Agents. J Polym Res. 2012;19(2):1–13.
20. Morgan PW. Interfacial Polymerization. Encyclopedia of Polymer Science and Technology: John Wiley & Sons, Inc.; 2002.
21. Pham QP, Sharma U, Mikos AG. Electrospinning of Polymeric Nanofibers for Tissue Engineering Applications: A Review. Tissue Eng. 2006;12(5):1197–211.
22. Zong X, Kim K, Fang D, Ran S, Hsiao BS, Chu B. Structure and Process Relationship of Electrospun Bioabsorbable Nanofiber Membranes. Polymer. 2002;43(16):4403–12.
23. Jarusuwannapoom T, Hongrojjanawiwat W, Jitjaicham S, Wannatong L, Nithitanakul M, Pattamaprom C, *et al.* Effect of Solvents on Electro-Spinnability of Polystyrene Solutions and Morphological Appearance of Resulting Electrospun Polystyrene Fibers. Eur Polym J. 2005;41(3):409–21.
24. Tsitlanadze G, Machaidze M, Kviria T, Djavakhishvili N, Chu CC, Katsarava R. Biodegradation of Amino-Acid-Based Poly (Ester Amide)s: *In Vitro* Weight Loss and Preliminary *in Vivo* Studies. J Biomater Sci Polym Ed. 2004;15(1):1–24.
25. Zamani M, Morshed M, Varshosaz J, Jannesari M. Controlled Release of Metronidazole Benzoate from Poly Epsilon-Caprolactone Electrospun Nanofibers for Periodontal Diseases. Eur J Pharm Biopharm. 2010;75(2):179–85.
26. Zeng J, Yang L, Liang Q, Zhang X, Guan H, Xu X, *et al.* Influence of the Drug Compatibility With Polymer Solution on the Release Kinetics of Electrospun Fiber Formulation. J Control Release. 2005;105(1–2):43–51.
27. Maretschek S, Greiner A, Kissel T. Electrospun Biodegradable Nanofiber Nonwovens for Controlled Release of Proteins. J Control Release. 2008;127(2):180–7.
28. Sy JC, Klemm AS, Shastri VP. Emulsion as a Means of Controlling Electrospinning of Polymers. Adv Mater. 2009;21(18):1814–9.
29. Yang Y, Li X, He S, Cheng L, Chen F, Zhou S, *et al.* Biodegradable Ultrafine Fibers With Core–Sheath Structures for Protein Delivery and its Optimization. Polym Adv Technol. 2011;22(12):1842–50.
30. Ritger PL, Peppas NA. A Simple Equation for Description of Solute Release I. Fickian and non-Fickian Release from non-Swellable Devices in the Form of Slabs, Spheres, Cylinders or Discs. J Control Release. 1986;5(1):23–36.
31. Baker SC, Southgate J. Towards Control of Smooth Muscle Cell Differentiation in Synthetic 3D Scaffolds. Biomaterials. 2008;29(23):3357–66.
32. Naruo K, Seko C, Kuroshima K, Matsutani E, Sasada R, Kondo T, *et al.* Novel Secretory Heparin-Binding Factors from Human Glioma Cells (Glia-Activating Factors) Involved in Glial Cell Growth. Purification and Biological Properties. J Biol Chem. 1993;268(4):2857–64.
33. Rubin JS, Chan AM, Bottaro DP, Burgess WH, Taylor WG, Cech AC, *et al.* A Broad-Spectrum Human Lung Fibroblast-Derived Mitogen is a Variant of Hepatocyte Growth Factor. Proc Natl Acad Sci. 1991;88(2):415–9.
34. Richardson WJ, Wilson E, Moore Jr JE. Altered Phenotypic Gene Expression of 10T1/2 Mesenchymal Cells in Nonuniformly Stretched PEGDA Hydrogels. Am J Physiol Cell Physiol. 2013;305(1):C100–110.
35. Horwitz JA, Shum KM, Bodle JC, Deng M, Chu CC, Reinhart-King CA. Biological Performance of Biodegradable Amino Acid-Based Poly (Ester Amide)s: Endothelial Cell Adhesion and Inflammation *In Vitro*. J Biomed Mater Res A. 2010;95(2):371–80.
36. Deng M, Wu J, Reinhart-King CA, Chu CC. Biodegradable Functional Poly (Ester Amide)s With Pendant Hydroxyl Functional Groups: Synthesis, Characterization, Fabrication and *In Vitro* Cellular Response. Acta Biomater. 2011;7(4):1504–15.
37. Lin S, Sandig M, Mequanint K. Three-Dimensional Topography of Synthetic Scaffolds Induces Elastin Synthesis by Human Coronary Artery Smooth Muscle Cells. Tissue Eng Part A. 2011;17(11–12):1561–71.
38. Carlson AL, Florek CA, Kim JJ, Neubauer T, Moore JC, Cohen RI, *et al.* Microfibrous Substrate Geometry as a Critical Trigger for Organization, Self-Renewal, and Differentiation of Human Embryonic Stem Cells Within Synthetic 3-Dimensional Microenvironments. Faseb J. 2012;26(8):3240–51.
39. Zhou L, Takayama Y, Boucher P, Tallquist MD, Herz J. LRP1 Regulates Architecture of the Vascular Wall by Controlling PDGFRÎ²-Dependent Phosphatidylinositol 3-Kinase Activation. PLoS One. 2009;4(9):e6922.
40. Hellstrom M, Kalen M, Lindahl P, Abramsson A, Betsholtz C. Role of PDGF-B and PDGFR-Beta in Recruitment of Vascular Smooth Muscle Cells and Pericytes During Embryonic Blood Vessel Formation in the Mouse. Development. 1999;126(14):3047–55.
41. Zhang H, Jia X, Han F, Zhao J, Zhao Y, Fan Y, *et al.* Dual-Delivery of VEGF and PDGF by Double-Layered Electrospun Membranes for Blood Vessel Regeneration. Biomaterials. 2012;34(9):2202–12.